Eur. Phys. J. D **64**, 287–296 (2011)
DOI: 10.1140/epjd/e2011-20227-8

THE EUROPEAN PHYSICAL JOURNAL D

Regular Article

A variational adiabatic hyperspherical finite element R matrix methodology: general formalism and application to H + H_2 reaction

M.N. Guimarães[1,2] and F.V. Prudente[1,a]

[1] Instituto de Física, Universidade Federal da Bahia, 40210-340 Salvador, BA, Brazil
[2] Centro de Formação de Professores, Universidade Federal do Recôncavo da Bahia, 45300-000 Amargosa, BA, Brazil

Received 21 April 2011 / Received in final form 25 June 2011
Published online 4 October 2011 –

Abstract. The aim of this paper is to present an efficient numerical procedure for the theoretical study of bimolecular reactions. It is based on the R matrix variational formalism and the p-version of the finite element method (p-FEM) for expanding the wave function in a finite basis set, and facilitates the development of an efficient algorithm to invert matrices that significantly reduces the computational time in R matrix calculations. We also utilise the self-consistent finite element method to optimise the elements mesh and provide faster convergence of results. We apply our methodology to the study of the collinear H + H_2 process and evaluate its efficiency by comparing our results with several results previously published in the literature.

1 Introduction

The study of scattering processes in the gas phase has interested researchers for many decades, as they are fundamental to our understanding of a huge range of physical phenomena. These range from atmospheric chemistry and the chemical combustion process, which both have important implications for the environment, to phenomena of astrophysical interest, such as those that occur in stellar media or the molecular collisions that take place in ultracold gases [1–5]. In an attempt to better understand the nature of these processes, progress in theoretical studies has made it possible to perform accurate calculations of the quantum dynamics within several systems (see Ref. [2] and references therein). This progress is due both to the development of new techniques and the emergence of powerful computers. A rather complicated case is that of bimolecular reactions. Such reactions have been the subject of numerous theoretical studies over the years, because, in addition to being important in various physical and chemical processes, many quantum effects have been found in cases of collisions at low energies [6].

The methodologies applied to the study of scattering problems of atoms and/or molecules fall into two categories; they either solve the time-dependent or the time-independent Schrödinger equation [6–8]. The studies that invoke the time-dependent method are based on temporal evolution of a wave packet calculated in a grid of points [8,9]. The advantage of this approach lies in its simpler implementation, permitting the treatment of systems involving a larger number of degrees of freedom. The disadvantage is that to obtain the full S matrix, it is necessary to propagate several wave packets. On the other hand, time-independent studies are frequently advantageous in the clarification of reaction mechanisms, the whole S matrix in a single calculation, however the coupling of a large number of vibrational and rotational states leads to considerable computational effort [3,7,8].

An important development in the theory of bimolecular reactions was the introduction of hyperspherical coordinate systems. In chemical physics and quantum chemistry, they have successfully been applied to scattering calculations using the reduced dimensionality approximation [10–12] and in full dimensions involving triatomic [13–17] and tetra-atomic molecules [18–23]. The hyperspherical coordinates are constituted by one hyperradius and a set of hyperangles that have the advantage of describing all channels evenly. Also, the Schrödinger equation for bimolecular reactions written in hyperspherical coordinates permits us to study the motion in the hyperradial coordinate independently of the hyperangular coordinates, treating the hyperradius as a slowly varying adiabatic variable.

Some methodologies that have also contributed to the recent progress in the study of quantum dynamics of chemical reactions are those based on R matrix theory [24,25]. This theory was introduced by Wigner and Eisenbud [26] to study nuclear reactions. Jackson [27] developed the variational approach based on the Hulthén-Kohn variational principle [28–30]. In chemical physics,

[a] e-mail: prudente@ufba.br

the variational R matrix method is applied to the study of electron-atom/molecule scattering [31,32], atom-diatom reactive scattering [33,34], photodissociation processes of triatomic molecules [35], unimolecular isomerisation reactions [36] and the two electronic states problem [37]. The principal features of the R matrix theory is that it is symmetric and real for real potentials. Moreover, it is easy to obtain the S matrix from the R matrix. In the R matrix approach, the major part of the computational work is done employing the real algebra, lessening the numerical effort.

A very accurate procedure which is applied in quantum mechanics combined with the variational formalism is the finite element method (FEM) [38]. The FEM is a general nomenclature for a set of variational numerical approaches that are based on the technique of space discretisation into elements and expansion of the wave function in terms of local polynomial basis functions defined in each of these elements. In the last years, the FEM has been utilised in the study of rovibrational bound states [39–42], reactive scattering processes [13,14,43–48] and the electronic structure of atoms and molecules [49–52]. There are two versions of the finite element method: the h-version uses polynomials of the same degree in all elements of the mesh, while the p-version allows one to use different degrees of polynomials in different elements and therefore is more flexible [40,53]. In particular, the p-version of the finite element method (p-FEM) has the advantage of making it possible to develop an efficient algorithm to invert the very large matrices encountered in scattering problems [47]. It reduces significantly the computational time and computer core memory requirement in the R matrix calculation.

In this paper we propose a general methodology based on the variational formulation of the R matrix theory in hyperspherical coordinates to study A + BC chemical reactions. In particular, the use of hyperspherical coordinates permits the adiabatic separation of the hyperangles and hyperradius variables in the sense of the well-known adiabatic separation of electronic and nuclear motions. The finite element method is then utilised to expand the wave function in the hyperradius direction, and an efficient matrix inversion technique, described in the Appendix, is used for the R matrix inversion. Then, in order to test our methodology, we calculate the reaction probabilities of the collinear $H + H_2 \rightarrow H_2 + H$ reaction. This reaction is a benchmark of bimolecular reactions and it is always utilised to test novel approaches [10–12,48,54–68].

This paper is organised as follows. In the next section we describe our theorical method for the treatment of an atom-diatom scattering problem: in Section 2.1 we present some systems of coordinates used in treating this problem; in Section 2.2 we formulate the variational R matrix theory in hyperspherical coordinates; in Section 2.3 we discuss the method of hyperspherical projection and in Section 2.4 we show the one-dimensional p-version of the finite element method. In Section 3 present and discuss our results for the collinear $H + H_2 \rightarrow H_2 + H$ reaction. The last section is dedicated to concluding remarks and the discussion avenues for future work.

2 Theory

We consider the collision between the atom A and the diatom BC, where the nuclei move with energy, E, which is below the complete dissociation energy. Thus, we confine our attention to chemical processes of the type

$$\mathrm{A} + \mathrm{BC}(\nu_I) \longrightarrow \begin{cases} \mathrm{A} + \mathrm{BC}(\nu_F) & \text{Channel I} \\ \mathrm{AB}(\nu_\mathrm{F}) + \mathrm{C} & \text{Channel II} \\ \mathrm{AC}(\nu_\mathrm{F}) + \mathrm{B} & \text{Channel III,} \end{cases} \tag{1}$$

where ν_I and ν_F are the rovibrational quantum numbers of reagents and products, respectively. Furthermore, we believe that the reaction occurs in a single adiabatic electronic state. Thus the hamiltonian of the triatomic system is given by

$$\widehat{H} = -\frac{\hbar^2}{2M_A}\nabla_A^2 - \frac{\hbar^2}{2M_B}\nabla_B^2 - \frac{\hbar^2}{2M_C}\nabla_C^2 + V(\mathbf{x}_A, \mathbf{x}_B, \mathbf{x}_C), \tag{2}$$

where $V(\mathbf{x}_A, \mathbf{x}_B, \mathbf{x}_C)$ is the potential energy surface in a specific electronic state.

2.1 Coordinate systems

In this subsection we present a brief description of the coordinate systems employed in our formalism. The choice of the coordinates is an important step in the study of molecular systems. In particular, we have utilised the mass weighed (scaled) Jacobi coordinates to treat the reactive scattering problem in the asymptotic region, while the hyperspherical coordinates are used to describe the molecular system within the interaction region. A review of various coordinate sets of triatomic molecular systems can be found in reference [69].

2.1.1 Mass weighed Jacobi coordinates

For a triatomic system there are three different sets of Jacobi vectors, each one represented by the relative vector between two bodies and the vector between their centre of mass and the third body; the center of mass vector is disregarded. The mass weighed Jacobi vectors $\mathbf{R}_\lambda$ and $\mathbf{r}_\lambda$, with $\lambda = I, II, III$ each representing one of the three channels in equation (1), are defined from the Jacobi ones in order to transform the three body problem into one that represents one particle with a reduced mass $\mu = (M_A M_B M_C / M)^{\frac{1}{2}}$ in a six-dimensional space.

Each set of mass weighed Jacobi vectors is suitable for expressing one particular channel under asymptotic conditions ($R_\lambda = |\mathbf{R}_\lambda| \longrightarrow \infty$). The asymptotic wave functions in each channel $\lambda = I, II, III$ can be written as

$$\Psi(\mathbf{R}_\lambda, \mathbf{r}_\lambda) = \sum_{j=1}^{n_\lambda} U_j(\mathbf{r}_\lambda) u_j(\mathbf{R}_\lambda), \tag{3}$$

where the asymptotic rovibrational states of a specific diatom, $U_j(\mathbf{r}_\lambda)$, are solutions of the three-dimensional Schrödinger equation

$$\left[-\frac{\hbar^2}{2\mu}\nabla^2_{\mathbf{r}_\lambda} + V\left(|\mathbf{R}_\lambda| \to \infty, \mathbf{r}_\lambda\right)\right] U_j(\mathbf{r}_\lambda) = E^\lambda_j U_j(\mathbf{r}_\lambda), \quad (4)$$

and $u_j(\mathbf{R}_\lambda)$ are plane waves as follows:

$$u_j(\mathbf{R}_\lambda) = C^{\text{in}}_j \frac{b_j}{\sqrt{k_j}} e^{-i\mathbf{k}_j\mathbf{R}_\lambda} - C^{\text{out}}_j \frac{b_j}{\sqrt{k_j}} e^{i\mathbf{k}_j\mathbf{R}_\lambda}. \quad (5)$$

In equation (5), $k_j = \sqrt{\frac{2\mu}{\hbar^2}(E - E_\lambda)}$, $b_j = 1$ or 0 if j represents an open ($E_\lambda < E$) or closed ($E_\lambda > E$) channel, respectively, and C^{in}_j and C^{out}_j are coefficients of the incoming and outgoing wave function, respectively.

2.1.2 Hyperspherical coordinates

In the region of strong interaction we use hyperspherical coordinates which are defined as a hyperradius, $\rho = \left(R^2_\lambda + r^2_\lambda\right)^{\frac{1}{2}}$ with $0 \leq \rho < \infty$, and five hyperangles, denoted collectively by Ω. Note that the hyperradius is independent of the arrangement set by the Jacobi coordinates, and the hyperangles can be defined in a variety of ways; see references [69,70] and references therein.

The use of hyperspherical coordinates permits the adiabatic separation of the hyperradius and the hyperangles variables. Thus, the wave function can be written as

$$\Psi(\rho, \Omega) = \rho^{-\frac{5}{2}} \sum_{j=1}^{n} h_j(\rho) g_j(\Omega, \rho) \quad (6)$$

where $g_j(\Omega, \rho)$ are eigenfunctions of the hyperangular equation for each value of the hyperradius:

$$\left[\frac{1}{2\mu\rho^2}\Lambda^2 + V(\rho, \Omega)\right] g_j(\Omega; \rho) = \varepsilon_j(\rho) g_j(\Omega; \rho), \quad (7)$$

where $\mathbf{\Lambda}$, the grand angular momentum operator, contains all the angular variables [71]. In equation (7) the eigenvalue $\varepsilon_j(\rho)$ represents the adiabatic curve associated with the jth hyperangle's state in the sense of the usual (known) adiabatic potential energy curves (surfaces) found in the adiabatic separation of electronic and nuclear motions.

There are several methods to efficiently solve equation (7) for the hyperangles, e.g. references [14,72–74], but this is not the purpose of this article, in which the central point is to solve for the hyperradial part.

2.2 Variational R matrix formalism

The variational formalism implies that we must first construct the functional of the energy for the triatomic system. This functional can be written, employing the matrix notation, as

$$J[\mathbf{h}] = \int_0^\infty d\rho \mathbf{h}^\dagger(\rho) \left\{-\frac{\hbar^2}{2\mu}\mathbf{1}\frac{d^2}{d\rho^2} + \widehat{\mathbf{A}}(\rho) + \mathbf{V}^{\text{ef}}(\rho) - E\right\} \times \mathbf{h}(\rho) \quad (8)$$

where

$$\{\widehat{\mathbf{A}}\}_{ij}(\rho) = -\frac{\hbar^2}{2\mu}\left[2A^{(1)}_{ij}(\rho)\frac{d}{d\rho} + A^{(2)}_{ij}(\rho)\right]$$

represents the elements of the non-adiabatic coupling matrix, with $A^{(1)}_{ij}(\rho) = \int d\Omega g^*_i(\Omega, \rho)\frac{\partial}{\partial\rho} g_j(\Omega, \rho)$ and $A^{(2)}_{ij}(\rho) = \int d\Omega g^*_i(\Omega, \rho)\frac{\partial^2}{\partial\rho^2} g_j(\Omega, \rho)$. The elements of the effective potential matrix are represented by

$$\{\mathbf{V}^{\text{ef}}\}_{ij}(\rho) = \left[\varepsilon_i(\rho) + 15\hbar^2/8\mu\rho^2\right]\delta_{ij}$$

and

$$\mathbf{h}^\dagger = (h^*_1(\rho), h^*_2(\rho), \ldots, h^*_n(\rho))$$

is the adjunct vector of the hyperradial functions.

The R matrix methodology relates the wave function with its normal derivative on the border of the surface between two regions into coordinate space: the outer region, or asymptotic region, and the interior region, or interaction region. In hyperspherical coordinates, the boundary surface between these two regions is defined only by $\rho = \rho_{max}$. Therefore, the boundary condition imposed by the variational R matrix formalism on the set of hyperradial functions and their normal derivatives is specified as

$$\mathbf{h}(\rho_{max}) = \mathbf{R}^{\text{h}} \left.\frac{d\mathbf{h}(\rho)}{d\rho}\right|_{\rho_{max}}, \quad (9)$$

where $\mathbf{R}^{\text{h}}$ is the hyperspherical R matrix. Thus, using the first Green's identity and condition (9) on the functional (8) we obtain a novel functional,

$$\begin{aligned} J[\mathbf{h}, \mathbf{h}'] = \int_0^{\rho_{max}} d\rho \Bigg\{ & \frac{\hbar^2}{2\mu}\frac{d\mathbf{h}^\dagger(\rho)}{d\rho}\frac{d\mathbf{h}(\rho)}{d\rho} \\ & + \mathbf{h}^\dagger(\rho)\left[\widehat{\mathbf{A}}(\rho) + \mathbf{V}^{\text{ef}}(\rho) - E\right]\mathbf{h}(\rho)\Bigg\} \\ & - \frac{\hbar^2}{2\mu}\left[\mathbf{h}^\dagger(\rho_{max})\mathbf{h}'(\rho_{max}) + \mathbf{h}'^\dagger(\rho_{max})\mathbf{h}(\rho_{max})\right] \\ & + \frac{\hbar^2}{2\mu}\mathbf{h}'^\dagger(\rho_{max})\mathbf{R}^h\mathbf{h}'(\rho_{max}), \end{aligned} \quad (10)$$

where $\mathbf{h}'(\rho_{max})$ is the derivative of $\mathbf{h}(\rho)$ at the point $\rho = \rho_{max}$.

The hyperspherical R matrix is found by expanding the hyperradial function vector in a known finite basis set $\{f_j\}$,

$$\mathbf{h}(\rho) = \sum_{j=1}^{p} \mathbf{f}_j(\rho)\mathbf{c}_j, \quad (11)$$

with

$$\mathbf{f}_j(\rho) = \begin{bmatrix} f_j(\rho) & & \mathbf{0} \\ & \ddots & \\ \mathbf{0} & & f_j(\rho) \end{bmatrix}_{n\times n} \quad \text{and} \quad \mathbf{c}_j = \begin{bmatrix} c_j^1 \\ \vdots \\ c_j^n \end{bmatrix}, \quad (12)$$

and by imposing the stationarity condition over the functional (10). Thus, the expression for the hyperspherical R matrix is obtained by solving the following matrix problem

$$\mathbf{R}^{\mathrm{h}} = \frac{\hbar^2}{2\mu}\mathbf{F}(\rho_{max})\left[\mathbf{H} - E\mathbf{O}\right]^{-1}\mathbf{F}^{\dagger}(\rho_{max}). \quad (13)$$

In equation (13) the following matrix notation is employed,

$$\{\mathbf{H} - E\mathbf{O}\}_{j,j'} = \int_0^{\rho_{max}} d\rho \Bigg\{ \frac{\hbar^2}{2\mu}\frac{d\mathbf{f}_j^{\dagger}(\rho)}{d\rho}\frac{d\mathbf{f}_{j'}(\rho)}{d\rho} + \mathbf{f}_j^{\dagger}(\rho)\left[\widehat{\mathbf{A}}(\rho) + \mathbf{V}^{\mathrm{ef}}(\rho) - E\right]\mathbf{f}_{j'}(\rho)\Bigg\},$$

$$\mathbf{F}(\rho) = \left[\mathbf{f}_1(\rho)\cdots\ \mathbf{f}_p(\rho)\right]$$

and

$$\mathbf{f}_j(\rho) = \mathbf{1}f_j(\rho),$$

where $\{\mathbf{H} - E\mathbf{O}\}_{j,j'}$ is a block of dimension $n\times n$ relative to the number of states in expression (6) and $\mathbf{F}(\rho)$ is a block row vector with dimension $n\times(n\times p)$.

The number of basis functions is crucial in defining the computational effort required to calculate the $\mathbf{H} - E\mathbf{O}$ matrix, as well as its inverse, in order to obtain the hyperspherical R matrix using equation (13). Therefore, it is essential that we employ efficient basis functions that reduce the memory required to store the array on a computer and the computational time to invert the array (see Sect. 2.4).

2.3 Hyperspherical projection

The asymptotic boundary conditions in mass weighed Jacobi coordinates are preferably expressed by taking the limit $R_\lambda \longrightarrow \infty$ for each channel $\lambda = I, II, III$. On the other hand, the region of strong interaction is better described in hyperspherical coordinates. As the boundary surface between regions is described using different coordinate systems, it is necessary to project the wave function defined around a hypersphere over a wave function defined on an appropriate Jacobi surface in order to obtain the scattering S matrix [75]. To this end, we are going to proceed to the analysis of the wave function at $\rho = \rho_{max}$ for larger values of ρ_{max}.

Taking $\rho \longrightarrow \rho_{max}$ sufficiently larger, we obtain the following Schrödinger equation in hyperspherical coordinates

$$\left[-\frac{\hbar^2}{2\mu}\mathbf{1}\frac{d^2}{d\rho^2} + \boldsymbol{\varepsilon}(\rho_{max})\right]\mathbf{h}(\rho) = E\mathbf{h}(\rho), \quad (14)$$

where $\{\boldsymbol{\varepsilon}(\rho_{max})\}_{ij} = \delta_{ij}\varepsilon_i(\rho_{max})$ and we assume that $\left.\frac{\partial g_i(\Omega,\rho)}{\partial\rho}\right|_{\rho_{max}} \approx 0 \implies A_{ij}^{(1)}(\rho_{max}) = A_{ij}^{(2)}(\rho_{max}) = 0$. Thus, the hyperradial functions can be expanded in terms of sine and cosine functions, such that

$$\mathbf{h}(\rho) = \mathbf{s}(\rho)\mathbf{a} + \mathbf{c}(\rho)\mathbf{b} \quad (15)$$

with $\mathbf{a}$ and $\mathbf{b}$ arbitrary vectors that depend on the asymptotic boundary conditions, and $\mathbf{s}$ and $\mathbf{c}$ are diagonal matrices whose elements are

$$\begin{cases} s_i(\rho) = \sin\left[k_i^+(\rho - \rho_{max})\right] \\ c_i(\rho) = \cos\left[k_i^+(\rho - \rho_{max})\right] \end{cases}$$

or

$$\begin{cases} s_i(\rho) = \sinh\left[k_i^-(\rho - \rho_{max})\right] \\ c_i(\rho) = \cosh\left[k_i^-(\rho - \rho_{max})\right] \end{cases}$$

for open and closed channels, respectively.

The hyperspherical projection requires that the right side of equations (3) and (6), and their normal derivatives, match on the surface $|\mathbf{R}_\lambda| = R_\lambda^{max} = \sqrt{\rho_{max}^2 - (r_\lambda^{eq})^2}$, with r_λ^{eq} the equilibrium distance of the specific diatom of channel λ. Since the Jacobi R matrix relates the vectors $\{\mathbf{u}(\mathbf{R}_\lambda^\infty)\}$ and their normal derivatives, it can be written as follows:

$$\mathbf{R}^{\mathrm{J}} = \left[\mathbf{I}^{(1)}\cdot\mathbf{X} + \mathbf{I}^{(2)}\right]\cdot\left[\frac{\partial}{\partial R_\lambda}\mathbf{I}^{(1)}\cdot\mathbf{X} + \frac{\partial}{\partial R_\lambda}\mathbf{I}^{(2)}\right]^{-1} \quad (16)$$

where

$$\mathbf{X} = -\left[\mathbf{s}(\rho_{max}) - \mathbf{R}^{\mathrm{h}}\frac{d}{d\rho}\mathbf{s}(\rho_{max})\right]^{-1} \times \left[\mathbf{c}(\rho_{max}) - \mathbf{R}^{\mathrm{h}}\frac{d}{d\rho}\mathbf{c}(\rho_{max})\right]$$

and $\{\mathbf{I}^{(i)}\}$ are matrices with blocks $\mathbf{I}_\lambda^{(i)}$ $(\lambda = I, II, III)$ of dimension $n_\lambda \times n$ whose elements are

$$\left\{\mathbf{I}_\lambda^{(1)}\right\}_{ij} = \int U_i^\lambda(\mathbf{r}_\lambda)\rho^{-\frac{5}{2}}s_j(\rho)g_j(\Omega,\rho)d\mathbf{r}_\lambda$$

$$\left\{\mathbf{I}_\lambda^{(2)}\right\}_{ij} = \int U_i^\lambda(\mathbf{r}_\lambda)\rho^{-\frac{5}{2}}c_j(\rho)g_j(\Omega,\rho)d\mathbf{r}_\lambda.$$

A desired asymptotic quantity in scattering problems is the S matrix whose mathematical relationship with the asymptotic wave function is given by

$$\mathbf{C}^{\mathrm{out}} = \mathbf{S}\mathbf{C}^{\mathrm{in}}, \quad (17)$$

where $\mathbf{C}^{\mathrm{in}}$ and $\mathbf{C}^{\mathrm{out}}$ are the vectors of incoming and outgoing coeficients, respectively. The transition probabilities between an incoming and an outgoing asymptotic state of the reaction are given by

$$P_{ij} = |S_{ij}|^2. \quad (18)$$

Considering function (5) on the surface $R_\lambda = R_\lambda^{max}$ and after some more algebraic manipulations, we find the S matrix is given by

$$\mathbf{S} = [(\mathbf{1} - i\mathbf{R})\mathbf{M}^*]^{-1}(\mathbf{1} + i\mathbf{R})\mathbf{M}, \quad (19)$$

where $\mathbf{M}$ is a block diagonal matrix with blocks $\mathbf{M}_\lambda$ ($\lambda = I, II, III$) whose elements are $\{\mathbf{M}_\lambda\}_{ij} = e^{-i\mathbf{k}_j \mathbf{R}_\lambda^\infty}\delta_{ij}$, and $\{\mathbf{R}\}_{ij} = \sqrt{k_i k_j}\left\{\mathbf{R}^{\mathrm{J}}\right\}_{ij}$ are the elements of the R matrix.

2.4 The p-version of the finite element method

The finite element method (FEM) has been described in detail in many other papers (e.g., see Refs. [40,47,50,76] and references therein), so here we limit ourselves to a brief introduction accentuating the more important characteristics for this study. The FEM in the one-dimensional case consists of two steps: (i) divide the integration interval $[a, b]$ into N_e elements, being the ith element defined in the range of q_{i-1} to q_i with $q_0 = a$ and $q_{N_e} = b$, and (ii) expand the wave function as follows

$$\Psi(q) = \sum_{i=1}^{N_e}\sum_{j=0}^{k_i} c_j^i f_j^i(q). \tag{20}$$

The basis functions $\{f_j^i(q)\}$ satisfy the following property

$$f_j^i(q) = 0 \quad \text{if} \quad q \notin [q_{i-1}, q_i], \tag{21}$$

the parameter k_i is the highest order of the basis functions associated with the ith element, $f_j^i(q)$ is the jth basis function of the same element and $\{c_j^i\}$ are the expansion coefficients. Consequently, using the FEM the elements of the matrix representation $\mathbf{B}$ of any operator $\widehat{B}$ have the following property:

$$B_{jj'}^{ii'} = \int_a^b dq f_j^i(q)\widehat{B}\ f_{j'}^{i'}(q) = 0 \quad \forall i \neq i'. \tag{22}$$

Note that this property leads to a very sparse matrix, concentrated on the diagonal and with a block structure.

In particular, the p-version of finite element method (p-FEM) utilises, as basis functions, two interpolant functions, $I_1^i \equiv f_0^i(q)$ and $I_2^i \equiv f_{k_i}^i(q)$, and shape functions, $S_j^i \equiv f_j^i(q)$ with $j = 1, \ldots, k_i - 1$ (see [50] for details). These basis functions have the important property that only the basis function $I_2^{N_e} \equiv f_{k_{N_e}}^{N_e}(q)$ is non-null on the last node of the mesh:

$$f_j^i(q_{N_e}) = \begin{cases} 1 \text{ for } i = N_e, & j = k_{N_e} \\ 0 & \text{otherwise.} \end{cases} \tag{23}$$

Due to properties (22) and (23), when we utilise the p-FEM for expanding the hyperradial wave functions (11), the hyperspherical R matrix (13) is written in the following form

$$\mathbf{R}^{\mathrm{h}} = \frac{\hbar^2}{2\mu}\left\{\mathbf{B}^{-1}\right\}^{N_e+1\ N_e+1}, \tag{24}$$

where $\mathbf{B} \equiv \mathbf{H} - E\mathbf{O}$ and the superscript indices in $\mathbf{B}^{-1}$ represent its last block. Therefore, we need to know only the last block of the inverse of $\mathbf{H} - E\mathbf{O}$ matrix to obtain the hyperspherical R matrix. This can be done efficiently utilising an algorithm developed by Prudente and Soares Neto, briefly described in paper [47] with a detailed discussion of its performance when applied to the study of a one-dimensional problem. This algorithm aims to calculate only the last block of the inverse matrix and is developed in detail in Appendix. It significantly reduces both the computational time to invert the matrix as well as the memory required to store it on the computer, since the resulting matrix is very sparse and the inversion procedure uses only the non-zero blocks of the array.

3 Results

In order to test our methodology we computed the transition probabilities for the collinear $\mathrm{H} + \mathrm{H}_2$ reaction on the LSTH potential energy surface [77]. The reduced mathematical dimensionality of the corresponding study transforms it into a bidimensional problem, with one hyperradius and one hyperangle. This simplicity permits a direct analysis of our methodology without the mathematical complexities of molecular rotations in the all-dimensional problem. We have compared our results with those obtained by other authors. In particular, we have employed polynomials of the same order for all elements ($k_i = k, \forall i$) in the p-FEM.

The adiabatic variational formulation of the problem employing hyperspherical coordinates permits us to carry out the calculation in separate steps. First, we diagonalised the matrix in order to find the eigenvalues and eigenfunctions of the hyperangular equation (7) for each value of hyperradius. For this we used the one-dimensional p-FEM with a recent modification to the procedure to build an optimised mesh for bound systems, as proposed by Prudente and Soares Neto [76]; this procedure was denominated the self-consistent finite element method (SC-FEM) [78]. The second step was determination of the hyperspherical R matrix (13) using the coupling terms and the effective potential obtained in the hyperangular problem. To do this, we used the p-FEM with a uniform mesh and the matrix inversion technique shown in Appendix. Thereafter we performed the hyperspherical projection to obtain the Jacobi R matrix (16). For that, the asymptotic vibrational states were also calculated using the p-FEM with an optimised mesh with the range $R_\lambda^{max} = \sqrt{\rho_{max}^2 - (r_\lambda^{eq})^2}$ and $r_\lambda^{max} = R_\lambda^{max}\mathrm{tg}(\frac{\theta_{max}}{2})$ for the two symmetric channels, where $r_e = 1.402$ bohr is the equilibrium distance of the H_2 molecule and $\theta_{max} = \arctan(\sqrt{3})$ is the maximum value of the hyperangle. In the calculations we have chosen 14 vibrational states for expanding the total wave function. Finally, the transition probabilities, $P_{\nu_I \nu_F}(E) = |S_{\nu_I \nu_F}|^2$, were computed from the S matrix given by expression (19).

We have also taken advantage of the symmetry of the problem to obtain the even and odd solutions of hyperangular equation separately. The p-FEM has been employed dividing the integration interval into equal halves and imposing conditions over the coeficients of expansion (20) in order to build symmetric and asymmetric basis functions.

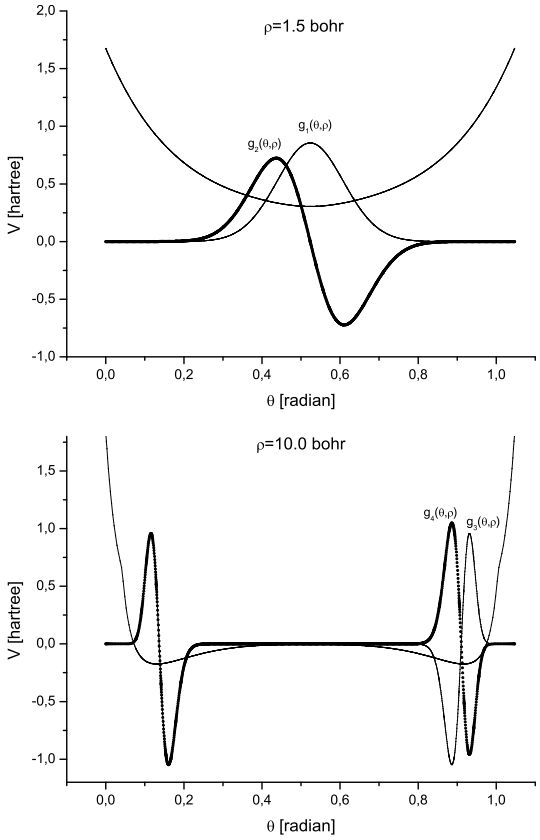

Fig. 1. Examples of symmetric and asymmetric hyperangular eigenfunctions for two values of the hyperradius for the $H + H_2$ system. The LSTH potential is drawn on the same figure.

Table 1. Selected reaction probability $P_{00}(E)$ at some energies, E, for $H + H_2$ on the LSTH potential energy surface as a function of ρ_{max} (in bohr) and N_e, with $k = 6$.

		$P_{00}(E)$			
ρ_{max}	N_e	0.5 eV	0.8 eV	1.1 eV	1.4 eV
10,0	50	0.083	0.938	0.292	0.058
	100	0.083	0.938	0.293	0.059
20,0	100	0.083	0.938	0.295	0.059
	200	0.083	0.938	0.295	0.060
30,0	150	0.083	0.938	0.295	0.060
	300	0.083	0.938	0.295	0.060
40,0	400	0.083	0.938	0.295	0.060
SKV*		(0.083)	(0.938)	(0.296)	(0.060)

* S matrix Kohn variational principle results [54–56].

In Figure 1 examples of symmetric and asymmetric hyperangular eigenfunctions for two hyperradius values are shown, with the potential drawn on the same figure.

In Table 1 we present the reaction probability $P_{00}(E)$ at four different energies to illustrate how convergence occurs when we increase ρ_{max} and the number of mesh elements, N_e, while keeping the number of basis functions in each element, k, identical for all ρ_{max} values. The reason for this is that when we increase k and maintain the $(\mathbf{H} - E\mathbf{O})$ dimension the results are essentially equal, but the computational time increases. Therefore, it is better to utilise a greater number of elements in the hyperradius direction than augmenting the k parameter; see the discussion in reference [47]. We also compare our results with accurate time-independent results [54–56] based on S matrix Kohn variational (SKV) principles. Note that the reaction probabilities for these energy values converges for the SKV results when ρ_{max} increases. Therefore, seeking a balance between accuracy and reduced computational time, we choose $\rho_{max} = 20$ bohr with the parameters $N_e = 200$ and $k = 6$ for the next calculations.

Table 2. Selected inelastic and reactive transition probabilities $(\nu_I \to \nu_F)$ at some energies, E, for the $H + H_2$ system on the LSTH potential energy surface. Our results were obtained with the p-FEM and use $\rho_{max} = 20$ bohr, $N_e = 200$ and $k = 6$.

Transition		E (eV)	Present	SKV*
Inelastic	$0 \to 0$	0.500	0.917	0.917
		1.100	0.171	0.172
		1.400	0.299	0.300
		0.800	6.17×10^{-2}	6.22×10^{-2}
	$1 \to 1$	1.100	0.123	0.123
		1.400	8.70×10^{-2}	8.74×10^{-2}
	$2 \to 2$	1.400	0.158	0.157
Reactive	$0 \to 1$	1.100	0.381	0.380
		1.400	0.225	0.224
		0.800	4.22×10^{-5}	3.74×10^{-5}
	$1 \to 1$	1.100	0.344	0.344
		1.400	0.304	0.305
	$0 \to 2$	1.400	0.107	0.107
	$1 \to 2$	1.400	0.125	0.126
	$2 \to 2$	1.400	0.482	0.482

* S matrix Kohn variational principle results [54–56].

To check the accuracy of our methodology, Table 2 shows some reactive and inelastic transition probabilities for different energy values. All results presented are in excellent agreement with accurate SKV results. The differences between our results and the SKV results are comparable with the differences between the SKV results and calculations utilising other methods such as the multiconfiguration time-dependent Hartree approximation [57], the time-independent wave packet formalism [55,56] and the time-dependent real wave packet formulation [59].

Finally, in Figures 2–4 the reactive probabilities are displayed as a function of energy for $\nu_I = 0 \to \nu_F = 0$, $\nu_I = 1 \to \nu_F = 0, 1$ and $\nu_I = 2 \to \nu_F = 0, 1, 2$ transitions, respectively. We compare them with the accurate results of Bondi and Connor [79] and demonstrate them to be in excellent agreement, even close to the resonance energies.

4 Concluding remarks

In this paper we have developed a general methodology based on the variational formulation of the R matrix theory, using hyperspherical coordinates to study the A + BC chemical reactions. This permitted the introduction of an adiabatic separation of the hyperangles and hyperradius variables in the sense of the well-known adiabatic

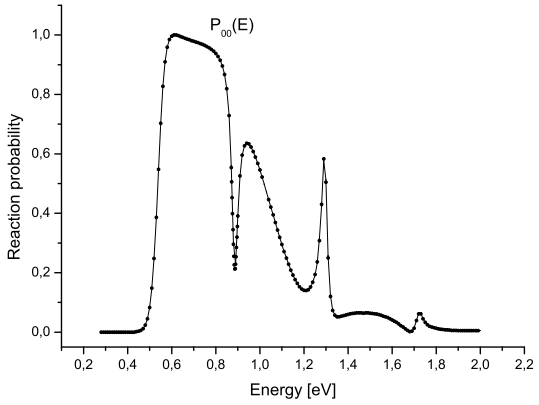

Fig. 2. Transition probability P_{00} as a function of the total energy, E, of the $H + H_2 \rightarrow H_2 + H$ collinear reaction. The solid line corresponds to the present work and the dots represent the accurate results from Bondi and Connor [79].

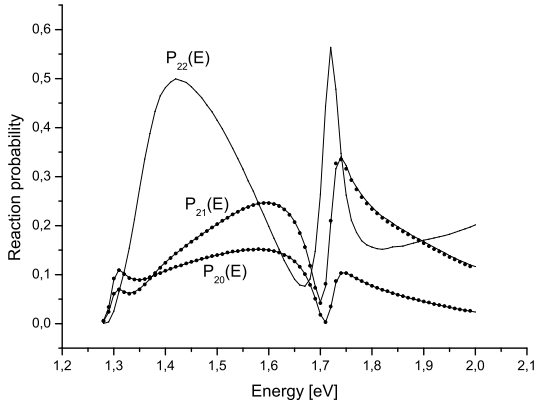

Fig. 4. Transition probabilities P_{20}, P_{21} and P_{22} as a function of total energy, E, of the $H + H_2 \rightarrow H_2 + H$ collinear reaction. The solid lines correspond to the present work and the dots represent the accurate results from Bondi and Connor [79].

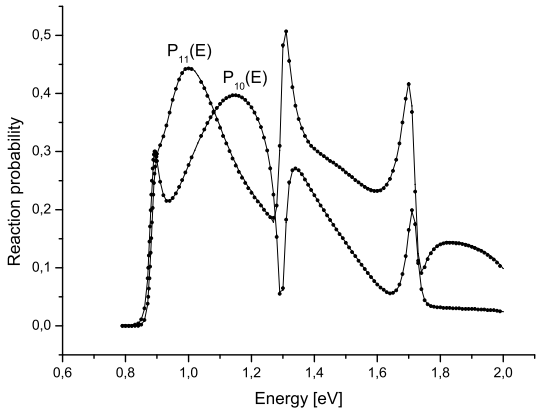

Fig. 3. Transition probabilities P_{10} and P_{11} as a function of total energy, E, of the $H + H_2 \rightarrow H_2 + H$ collinear reaction. The solid lines correspond to the present work and the dots represent the accurate results from Bondi and Connor [79].

separation of electronic and nuclear motions. Moreover, the p-version of the finite element method (p-FEM) was utilised to expand the wave function in the hyperradius direction. Using the properties of p-FEM we implemented an efficient algorithm for the R matrix inversion based on the matrix inversion technique developed by Prudente and Soares Neto [47]. This algorithm allows the matrix inversion procedure to be done using small blocks of the matrix, and only the non-zero blocks of the matrix need to be kept in the computer memory.

The advantage of our methodology is that it reduces the computational effort required for the matrix inversion, which is usually higher in the variational approach, by employing a procedure of inversion by blocks. For example, the CPU time required to perform the linear algebra calculations and the size of the core memory required to store the matrix elements in this procedure scales linearly with the number of elements, N_e, in the hyperradius mesh, as shown in reference [47]. Thus, our proposed methodology keeps some similarities with the usual propagation methods (close coupling treatment) for multichannel problems, although it is based on the variational principle.

Note that the matrices **H** and **O** in equations (13) and (24) need only be constructed once and then saved in computer memory they can then be used to calculate the scattering information at any total energies. Moreover, the methodology permits determination of all probabilities of reactive and inelastic transitions in a single calculation for each energy, as distinct from the time-dependent methods where it is usually necessary to perform several wave packet propagations. Another advantage of the present procedure is that the p-FEM can be applied to a variety of systems without the need for new trial basis functions for both the hyperradial and hyperangular parts of the problem.

As a rigorous test of our methodology, we calculated the inelastic and reactive transition probabilities for the collinear $H + H_2$ reaction on the LSTH potential energy surface. Our results are in excellent agreement with those obtained by others groups using different methods. In particular, we cited the accurate time-independent results based on the S matrix Kohn variational principles and those obtained by Bondi and Connor using the R matrix propagation technique.

The achievements of this work are representative of our aim in this research field: the construction of a computational code based on this novel time-independent variational methodology that is able to carry through extensive atom-diatom reactive scattering calculations as, for example, the ones developed by Hankel et al. [80] based on a time-dependent methodology, and Skouteris et al. [81] with a time-independent coupled-channel procedure. In meeting our aim is that we intend to employ the present approach to study other triatomic systems besides the collinear $H + H_2$ reaction.

Currently, we are working towards extending the code to treat the atom-diatom reaction considering its full dimensionality. In this new computational implementation some strategies will be evaluated to solve the hyperangular

problem posed by equation (7), such as the finite element method, the hyperquantisation algorithm developed by Aquilanti et al. [72,73] or the use of $\mathscr{Y}$ functions as proposed by Launay [74]. Then, we will reduce the dimension of the problem by treating the hyperradius as an adiabatic variable to obtain equation (13), after which we will employ the p-FEM to treat the hyperradial part and enable the implementation of the efficient matrix inversion technique to solve equation (24).

Another extension of our methodology that we plan to implement in the near future is to consider reactions that involve multiple electronic states with non-adiabatic couplings. For example, to study a collinear reaction within a diabatic framework, small modifications to our code will be necessary, especially in the hyperangular step (Eq. (7)). Initial tests will be performed on a collinear model of the $H + H_2$ reaction [82,83].

The authors thank J.J. Soares Neto for helpful discussions and are very grateful to H.-D. Meyer for providing the Bondi and Connor reactive scattering data (Ref. [79]). This work has been supported by the following Brazilian National Research Councils: Conselho Nacional de Desenvolvimento Científico e Tecnológico (CNPq), Coordenação de Aperfeiçoamento de Pessoal de Nível Superior (CAPES) and Fundação de Amparo a Pesquisa do Estado da Bahia (FAPESB).

Appendix: Matrix inversion technique

In this appendix we illustrate a technique to invert the $\mathbf{B} \equiv \mathbf{H} - E\mathbf{O}$ matrix required to obtain the hyperspherical R matrix given by equation (13). In the finite element notation, the matrix $\mathbf{B}$ of any local operator $\widehat{B}$ has the following general form (see Eq. (22)):

$$\mathbf{B} = \begin{bmatrix} \mathbf{B}^1 & \mathbf{b}^1 & \mathbf{0} & \mathbf{0} & \cdots & \mathbf{0} \\ (\mathbf{b}^1)^\dagger & \mathbf{B}^2 & \mathbf{b}^2 & \mathbf{0} & \cdots & \mathbf{0} \\ \mathbf{0} & (\mathbf{b}^2)^\dagger & \mathbf{B}^3 & \mathbf{b}^3 & \ddots & \vdots \\ \mathbf{0} & \mathbf{0} & (\mathbf{b}^3)^\dagger & \ddots & \ddots & \mathbf{0} \\ \vdots & \vdots & \ddots & \ddots & \mathbf{B}^{N_e} & \mathbf{b}^{N_e} \\ \mathbf{0} & \mathbf{0} & \cdots & \mathbf{0} & (\mathbf{b}^{N_e})^\dagger & \mathbf{B}^{N_e+1} \end{bmatrix}, \quad \text{(A.1)}$$

where

$$\mathbf{B}^i = \begin{bmatrix} B^{i-1}_{k_i\ k_i} + B^i_{0\ 0} & B^i_{0\ 1} & \cdots & B^i_{0\ k_i-1} \\ B^i_{1\ 0} & B^i_{1\ 1} & \cdots & B^i_{1\ k_i-1} \\ \vdots & \vdots & \ddots & \vdots \\ B^i_{k_i-1\ 0} & B^i_{k_i-1\ 1} & \cdots & B^i_{k_i-1\ k_i-1} \end{bmatrix}, \quad \text{(A.2)}$$

$$\mathbf{b}^i = \begin{bmatrix} B^i_{0\ k_i} & 0 \cdots 0 \\ B^i_{1\ k_i} & 0 \cdots 0 \\ \vdots & \vdots \ddots \vdots \\ B^i_{k_i-1\ k_i} & 0 \cdots 0 \end{bmatrix} \quad \text{(A.3)}$$

with $i = 1, \ldots N_e$ and $\mathbf{B}^{N_e+1} = B^{N_e}_{k_{N_e}\ k_{N_e}}$. The $\mathbf{B}$ inverse has the following structure:

$$\mathbf{C} = \mathbf{B}^{-1} = \begin{bmatrix} \mathbf{C}^{1\ 1} & \mathbf{C}^{1\ 2} & \cdots & \mathbf{C}^{1\ N_e+1} \\ \mathbf{C}^{2\ 1} & \mathbf{C}^{2\ 2} & \cdots & \mathbf{C}^{2\ N_e+1} \\ \vdots & \vdots & \ddots & \vdots \\ \mathbf{C}^{N_e+1\ 1} & \mathbf{C}^{N_e+1\ 2} & \cdots & \mathbf{C}^{N_e+1\ N_e+1} \end{bmatrix}. \quad \text{(A.4)}$$

Using property (23) in expression (14), we find that the $\mathbf{F}$ vector on the surface defined by $\rho = \rho_{max}$ becomes:

$$\mathbf{F}(q_{N_e} = \rho_{max}) = \begin{bmatrix} \mathbf{0}\ \mathbf{0} \cdots \mathbf{1} \end{bmatrix}. \quad \text{(A.5)}$$

Then, the hyperspherical R matrix (Eq. (13)) is transformed in the expression (24). We show that the inversion process aims to calculate only the last block, $\mathbf{C}^{N_e+1\ N_e+1}$, of the $\mathbf{C} = \mathbf{B}^{-1}$ matrix.

A.1 Matrix partition method

Our matrix inversion procedure is based on the matrix partition method of Löwding and Feshbach algebra [84]. The partition method divides the original matrix into submatrices and its inverse into the following form:

$$\mathbf{X} = \begin{bmatrix} \mathbf{X}_{11}\ \mathbf{X}_{12} \\ \mathbf{X}_{21}\ \mathbf{X}_{22} \end{bmatrix} \implies \mathbf{Y} = \mathbf{X}^{-1} = \begin{bmatrix} \mathbf{Y}_{11}\ \mathbf{Y}_{12} \\ \mathbf{Y}_{21}\ \mathbf{Y}_{22} \end{bmatrix}, \quad \text{(A.6)}$$

where $\mathbf{X}_{11}$ and $\mathbf{X}_{22}$ are square and non-singular submatrices, and the submatrices of $\mathbf{Y}$ have the same dimension as the submatrices of $\mathbf{X}$ with the same indices. Using the relation $\mathbf{X} \cdot \mathbf{Y} = \mathbf{1}$ and straightforward algebraic manipulations, we find the submatrices of $\mathbf{Y}$ whose last block is (see Ref. [85] for details):

$$\mathbf{Y}_{22} = \left(\mathbf{X}_{22} - \mathbf{X}_{21}\mathbf{X}_{11}^{-1}\mathbf{X}_{12}\right)^{-1}. \quad \text{(A.7)}$$

The original problem is thus reduced to that of finding the inverse of $\mathbf{X}_{11}$ and $\left(\mathbf{X}_{22} - \mathbf{X}_{21}\mathbf{X}_{11}^{-1}\mathbf{X}_{12}\right)$. In particular we are interested in the special case in which $\mathbf{X}_{12}$ and $\mathbf{Y}_{12}$ are block column vectors, $\mathbf{X}_{21}$ and $\mathbf{Y}_{21}$ are block row vectors, and, $\mathbf{X}_{22}$ and $\mathbf{Y}_{22}$ are square matrices.

A.2 Block inversion procedure

Now we apply the block inversion procedure to compute the last block of the $\mathbf{C}$ matrix, defined as $\mathbf{Y}_{22}^{N_e+1} = \mathbf{C}^{N_e+1\ N_e+1}$, given by

$$\begin{aligned} \mathbf{Y}_{22}^{N_e+1} &= \left(\mathbf{X}_{22} - \mathbf{X}_{21}\mathbf{X}_{11}^{-1}\mathbf{X}_{12}\right)^{-1} \\ &= \left(\mathbf{B}^{N_e+1} - (\mathbf{b}^{N_e})^\dagger \mathbf{Y}_{22}^{N_e} \mathbf{b}^{N_e}\right)^{-1}, \end{aligned} \quad \text{(A.8)}$$

where

$$\mathbf{X}_{11} = \begin{bmatrix} \mathbf{B}^1 & \mathbf{b}^1 & \mathbf{0} & \cdots & \mathbf{0} \\ (\mathbf{b}^1)^\dagger & \mathbf{B}^2 & \mathbf{b}^2 & \ddots & \vdots \\ \mathbf{0} & (\mathbf{b}^2)^\dagger & \ddots & \ddots & \mathbf{0} \\ \vdots & \ddots & \ddots & \mathbf{B}^{N_e-1} & \mathbf{b}^{N_e-1} \\ \mathbf{0} & \cdots & \mathbf{0} & (\mathbf{b}^{N_e-1})^\dagger & \mathbf{B}^{N_e} \end{bmatrix} \quad \text{(A.9)}$$

and $\mathbf{Y}_{22}^{N_e}$ is the last block of the inverse matrix of $\mathbf{X}_{11}$. Using the partition method again, the $\mathbf{Y}_{22}^{N_e}$ block is given by

$$\begin{aligned}\mathbf{Y}_{22}^{N_e} &= \left(\mathbf{X}_{22} - \mathbf{X}_{21}\mathbf{X}_{11}^{-1}\mathbf{X}_{12}\right)^{-1} \\ &= \left(\mathbf{B}^{N_e} - (\mathbf{b}^{N_e-1})^{\dagger}\mathbf{Y}_{22}^{N_e-1}\mathbf{b}^{N_e-1}\right)^{-1}, \quad \text{(A.10)}\end{aligned}$$

where we redefined

$$\mathbf{X}_{11} = \begin{bmatrix} \mathbf{B}^1 & \mathbf{b}^1 & \mathbf{0} & \cdots & \mathbf{0} \\ (\mathbf{b}^1)^{\dagger} & \mathbf{B}^2 & \mathbf{b}^2 & \ddots & \vdots \\ \mathbf{0} & (\mathbf{b}^2)^{\dagger} & \ddots & \ddots & \mathbf{0} \\ \vdots & \ddots & \ddots & \mathbf{B}^{N_e-2} & \mathbf{b}^{N_e-2} \\ \mathbf{0} & \cdots & \mathbf{0} & (\mathbf{b}^{N_e-2})^{\dagger} & \mathbf{B}^{N_e-1} \end{bmatrix} \quad \text{(A.11)}$$

and $\mathbf{Y}_{22}^{N_e-1}$ is the last block of the inverse matrix of $\mathbf{X}_{11}$ redefined. Note that to obtain the $\mathbf{Y}_{22}^{i}$ block it is necessary to calculate the $\mathbf{Y}_{22}^{i-1}$ block. The general expression is the following:

$$\mathbf{Y}_{22}^{i} = \left(\mathbf{B}^{i} - (\mathbf{b}^{i-1})^{\dagger}\mathbf{Y}_{22}^{i-1}\mathbf{b}^{i-1}\right)^{-1}, \quad \text{(A.12)}$$

with $\mathbf{Y}_{22}^{1} = (\mathbf{B}^1)^{-1}$.

Thus, the procedure to obtain the last block of the inverse matrix of $\mathbf{B} = \mathbf{H} - E\mathbf{O}$ is the following:

1. We invert the $\mathbf{B}^1$ block and obtain $\mathbf{Y}_{22}^{1}$;
2. Using equation (A.12), we calculate the $\mathbf{Y}_{22}^{i}$ blocks until we obtain the $\mathbf{Y}_{22}^{N_e}$ block;
3. Using equation (A.8), we calculate the $\mathbf{C}^{N_e}+1$ N_e+1 matrix block (last block of the inverse of the $\mathbf{B}$ matrix).

References

1. *Molecular Astrophysics: State of the Art and Future Directions*, edited by G.H.F. Diercksen, W.F. Huebner, P.W. Langhoff (D. Reidel, Dordrecht, 1985)
2. *Dynamics of Molecules and Chemical Reactions*, edited by R.E. Wyatt, J.Z.H. Zhang (Dekker, New York, 1996)
3. S.C. Althorpe, D.C. Clary, Ann. Rev. Phys. Chem. **54**, 493 (2003)
4. J.M. Hutson, P. Soldán, Int. Rev. Phys. Chem. **26**, 1 (2007)
5. D.C. Clary, Science **321**, 789 (2008)
6. G. Nyman, H.-G. Yu, Rep. Prog. Phys. **60**, 1001 (2000)
7. W. Hu, G.C. Schatz, J. Chem. Phys. **125**, 132301 (2006)
8. G.G. Balint-Kurti, Int. Rev. Phys. Chem. **27**, 507 (2008)
9. F.V. Prudente, J.M.C. Marques, A.M. Maniero, Chem. Phys. Lett. **474**, 18 (2009)
10. A. Kuppermann J.A. Kaye, J.P. Dwyer, Chem. Phys. Lett. **74**, 257 (1980)
11. J. Römelt, Chem. Phys. Lett. **74**, 263 (1980)
12. D.K. Bondi, J.N.L. Connor, Chem. Phys. Lett. **92**, 570 (1982)
13. A. Kuppermann, P.G. Hipes, J. Chem. Phys. **84**, 5963 (1986)
14. R.T. Pack, G.A. Parker, J. Chem. Phys. **87**, 3888 (1987)
15. J.M. Launay, M. Le Dourneuf, Chem. Phys. Lett. **163**, 178 (1989)
16. J.M. Launay, M. Le Dourneuf, Chem. Phys. Lett. **169**, 473 (1990)
17. J. Linderberg, S.B. Padkjær, Y. Öhrn, B. Vessal, J. Chem. Phys. **90**, 6254 (1989)
18. Y. Öhrn, J. Linderberg, Mol. Phys. **49**, 53 (1983)
19. X. Chapuisat, Mol. Phys. **72**, 1233 (1991)
20. A. Kuppermann, in *Advances in Molecular Vibrations and Collision Dynamics* (J.M. Bowman, JAI Press, Greenwich/London, 1994), Vol. 2B, p. 117
21. V. Aquilanti, G. Capecchi, S. Cavalli, Adv. Quantum Chem. **36**, 342 (1999)
22. V. Aquilanti, S. Cavalli, J. Chem. Soc., Faraday Trans. **93**, 802 (1997)
23. S.K. Pogrebnya, J. Echave, D.C. Clary, J. Chem. Phys. **107**, 8975 (1997)
24. J.C. Light, in *Theory of Chemical Reactions Dynamics* (D.C. Clary, D. Reidel, Dordrecht, 1986), p. 215
25. H. Le Rouzo, Am. J. Phys. **71**, 273 (2003)
26. E.P. Wigner, L. Eisenbud, Phys. Rev. **72**, 29 (1947)
27. J.L. Jackson, Phys. Rev. **83**, 301 (1951)
28. L. Hulthén, K. Fysiograf. Sällsk. Lund Förhandl **14**, 257 (1944)
29. L. Hulthén, Ark. Mat. Astron. Fys. A **35** (1948)
30. W. Kohn, Phys. Rev. **74**, 1763 (1948)
31. C.W. McCurdy, T.N. Rescigno, B.I. Schneider, Phys. Rev. A **36**, 2061 (1987)
32. B.I. Schneider, Chem. Phys. Lett. **31**, 237 (1975)
33. J. Linderberg, Int. J. Quant. Chem. **35**, 801 (1989)
34. J. Linderberg, Comp. Phys. Rep. **6**, 209 (1987)
35. J.J. Soares Neto, J. Linderberg, J. Chem. Phys. **95**, 8022 (1991)
36. J. Linderberg, J. Chem. Soc., Faraday Trans. **93**, 893 (1997)
37. J. Linderberg, Adv. Quantum Chem. **32**, 315 (1998)
38. L.R. Ram-Moham, *Finite Element and Boundary Element Applications in Quantum Mechanics* (Oxford University Press, New York, 2002)
39. R. Jaquet, Comput. Phys. Commun. **58**, 257 (1990)
40. J.J. Soares Neto, F.V. Prudente, Theor. Chim. Acta **89**, 415 (1994)
41. T.J. Dudley, R.R. Pandey, P.E. Staffin, M.R. Hoffmann, G.C. Schatz, J. Chem. Phys. **114**, 6166 (2001)
42. M. Salci, S.B. Levin, N. Elander, E. Yarevsky, J. Chem. Phys. **129**, 134304 (2008)
43. R. Jaquet, Theor. Chim. Acta. **71**, 425 (1987)
44. R. Jaquet, Chem. Phys. **118**, 17 (1987)
45. J. Linderberg, B. Vessal, Int. J. Quant. Chem. **31**, 65 (1987)
46. G.A. Parker, R.T. Pack, B.J. Archer, R.B. Walker, Chem. Phys. Lett. **137**, 564 (1987)
47. F.V. Prudente, J.J. Soares Neto, Chem. Phys. Lett. **309**, 471 (1999)
48. O. Chuluunbaatar, A.A. Gusev, M.S. Kaschiev, V.A. Kaschieva, A. Amaya-Tapia, S.Y. Larsen, S.I. Vinitsky, J. Phys. B At. Mol. Opt. Phys. **39**, 243 (2006)
49. J.E. Pask, B.M. Klein, P.A. Sterne, C.Y. Fong, Comput. Phys. Commun. **135**, 1 (2001)
50. M.N. Guimarães, F.V. Prudente, J. Phys. B At. Mol. Opt. Phys. **38**, 2811 (2005)
51. L. Yang, D. Heinemann, D. Kolb, Chem. Phys. Lett. **192**, 499 (1992)
52. R. Alizadegan, K.J. Hsia, T.J. Martinez, J. Chem. Phys. **132**, 034101 (2010)

53. J.J. Soares Neto, J. Comput. Chem. **15**, 144 (1994)
54. D.T. Colbert, W.H. Miller, J. Chem. Phys. **96**, 1982 (1992)
55. S.C. Althorpe, D.J. Kouri, D.K. Hoffman, J.Z.H. Zhang, J. Chem. Soc., Faraday Trans. **93**, 703 (1997)
56. Y. Huang, S.S. Iyengar, D.J. Kouri, D.K. Hoffman, J. Chem. Phys. **105**, 927 (1996)
57. A. Jäckle, H.-D. Meyer, J. Chem. Phys. **102**, 5605 (1995)
58. B. Poirier, W.H. Miller, Chem. Phys. Lett. **265**, 77 (1997)
59. S.K. Gray, G.G. Balint-Kurti, J. Chem. Phys. **108**, 950 (1998)
60. S. Li, G. Li, H. Guo, J. Chem. Phys. **115**, 9637 (2001)
61. H. Zhang, S.C. Smith, J. Chem. Phys. **120**, 1161 (2004)
62. H. Han, P. Brumer, J. Chem. Phys. **122**, 144316 (2005)
63. C. Venkataraman, W.H. Miller, J. Chem. Phys. **126**, 094104 (2007)
64. L.R. Pettey, R.E. Wyatt, J. Phys. Chem. A **112**, 13335 (2008)
65. R.R. Khorasani, R.S. Dumont, J. Chem. Phys. **129**, 034110 (2008)
66. B. Poirier, J. Chem. Phys. **129**, 084103 (2008)
67. H. Schwetlick, J. Zimmer, J. Chem. Phys. **130**, 124106 (2009)
68. A. Goussev, R. Schubert, H. Waalkens, S. Wiggins, J. Chem. Phys. **131**, 144103 (2009)
69. M. Ragni, A.C.P. Bitencourt, V. Aquilanti, Prog. Theor. Chem. Phys. **16**, 133 (2007)
70. A. Kuppermann, J. Phys. Chem. **100**, 2621 (1996)
71. F.T. Smith, Phys. Rev. **120**, 1058 (1960)
72. V. Aquilanti, S. Cavalli, D. De Fazio, J. Chem. Phys. **109**, 3792 (1998)
73. V. Aquilanti, S. Cavalli, D. De Fazio, A. Volpi, A. Aguilar, X. Gimenez, J.L. Maria, J. Chem. Phys. **109**, 3805 (1998)
74. J.M. Launay, Theor. Chim. Acta **79**, 183 (1991)
75. R.B. Walker, E.F. Haynes, in *Theory of Chemical Reactions Dynamics* (D.C. Clary, D. Reidel, Dordrecht, 1986), p. 105
76. F.V. Prudente, J.J. Soares Neto, Chem. Phys. Lett. **302**, 43 (1999)
77. D.G. Thuhlar, C.J. Horowitz, J. Chem. Phys. **68**, 2466 (1978)
78. E.M. Nascimento, F.V. Prudente, M.N. Guimarães, A.M. Maniero, J. Phys. B At. Mol. Opt. Phys. **44**, 015003 (2011)
79. D.K. Bondi, J.N.L. Connor, J. Chem. Phys. **82**, 4383 (1985)
80. M. Hankel, S.C. Smith, S.K. Gray, G.G. Balint-Kurti, Comput. Phys. Commun. **179**, 569 (2008)
81. D. Skouteris, J.F. Castillo, D.E. Manolopoulos, Comput. Phys. Commun. **133**, 128 (2000)
82. C. Shin, S. Shin, J. Chem. Phys. **113**, 6528 (2000)
83. H. Nakamura, J. Phys. Chem. A **110**, 10929 (2006)
84. T. Seideman, J. Chem. Phys. **98**, 1989 (1993)
85. G.G. Hall, *Matrices and Tensors* (Pergamon Press, Oxford, 1963)